Research Paper
International Journal of Aerospace System Engineering
Vol.8, No.1, pp.1-13 (2021)

ISSN 2383-4986
EISSN 2508-7169
http://dx.doi.org/10.20910/IJASE.2021.8.1.1

Structure and Vibration Analyses of Low Speed Contra-Rotating Fan Stage with High Aspect Ratio

Supen Kumar Sah†, Anup Ghosh, Chetan S Mistry
Department of Aerospace Engineering
Indian Institute of Technology Kharagpur, India

Abstract

Contra-rotating fan is comprised of two rotors which are rotating in the opposite direction. The fan stages are named rotor-1 and rotor-2. Benefits from the use of contra rotation are in terms of better efficiency and improved thrust to weight ratio. Failure of contra-rotating fan stage blade in-service results in safety risks, repair costs, and revenue losses. This paper focuses on the vibration analysis and one way fluid-structure interaction of high aspect ratio, low speed contra-rotating fan rotors. Modal analysis and modal pre-stress analysis of contra-rotating fan rotors were carried out to calculate the natural frequencies, One way fluid-structure interaction (FSI) was carried out where the computational analysis of the blades was performed using ANSYS CFX. The boundary conditions for CFD analysis were considered from the actual experimental velocity flow field at the inlet and pressure outlet. Based on the results obtained from the CFD analysis, the structural analysis such as deformation and Von-Misses stresses was carried out by using the finite element method (FEM) with ANSYS. The results provide necessary guidelines for the safe running of the contra-rotating fan. The analysis also will be helpful to understand the change of flow behavior due to a rotor deformation.

Key Words : Conta-Rotating Fan Stage**,** One way FSI, Blade Vibration, Modal Analysis, Modal Pre-stress Analysis

1. Introduction

Turbomachines like compressors, turbines, and fans are the main components of gas turbine engines. The development of modern aircraft fan/compressor demands for reduction of specific fuel consumption, efficiency, and improvement in performance which demands an increase in bypass ratio. A high bypass ratio leads to an increase in engine weight and installation drag. The contra-rotating fan stage is comprised of two rotors that are rotating in the opposite direction. Benefits from the use of contra rotation are in terms of better efficiency and improved thrust to weight ratio, which is an important criterion for both military and commercial aircraft. In comparison with an ordinary axial flow fan, the contra-rotating fan has characteristics like compact structure, high pressure ratio, high flow rate, and high efficiency [1-2], etc. Contra-rotating fan rotors are designed at a high aspect ratio which leads to smaller chord length and smaller passage area for diffusion. Contra rotating fan stage performance is significantly affected by the speed ratio of two rotors, the axial gap between them [3], and tip clearance [4].

The interaction between fluid and structure takes place in various engineering fields. Fluid-structure interaction (FSI) analysis is a multi physics problem, which is distinguished, that the fluid flow around the body has a strong impact on the structure, and vice versa. A multi physics problem involves fluid and structural dynamics, which are described by the relations of continuum mechanics. FSI simulation has been divided into monolithic and partitioned methods [5]. This paper will focus only on the partitioned methods. Information on monolithic and partitioned methods is available in the literature [6]. In the partitioned approach, the interaction between two different physics phenomena has been performed in separate analyses. From the perspective of the mechanical application, the FSI analysis consists of performing structural analysis. The pressure load achieved from a CFD analysis can be used to investigate the structural response of rotors. The interaction analysis between the fluid and the

Received: Oct. 13, 2018 Revised: May 06, 2021 Accepted: May 14, 2021
† Corresponding Author
Tel: +91-89-4696-3336, E-mail: supen146@gmail.com

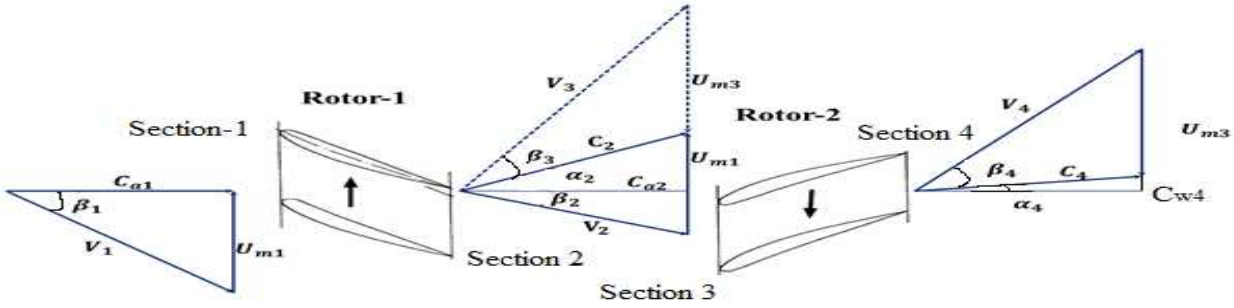

Figure 1 Velocity triangle

structure typically takes place at the boundaries that the mechanical model shares with the fluids model. These boundaries of interaction are called as the fluid-structure interface. It is the interface where the results of one analysis are passed to the other one as the loads.

In this paper, one way FSI model of contra-rotating fan stage has been developed with CFD for a fluid and FEM for structural analysis in terms of Von Misses stress and deformation. The finite element, the modal analysis of fan rotors is also performed to determine its natural frequencies. Determination of natural frequencies, mode shapes, and location of nodes can be visually examined for existing setup as well as design improvements of the geometrically and aerodynamically twisted blades. A commercially available finite element analysis (FEA) tool ANSYS is used to model and solve the response characteristics of rotors. One way FSI has been carried out with the which pressure load is imported from the CFD simulation to the FEA simulation. Further using the imported load the deformation and Von-Misses stress distribution in the blade are studied.

2. Design of Contra Rotating Fan Blade

The contra-rotating rotor-1 and rotor-2 were designed based on a variable work loading at different 20 blade sections to get the desired pressure rise. It was assumed that rotor-2 receives air at an absolute velocity and discharges axially. The whirl component from the rotor-1 transfers to the rotor-2 which is rotating in opposite direction and forces the rotor-2 to work additionally, thereby resulting advantage in terms of higher relative velocity at the rotor-2 inlet as shown in Figure-1. The axial velocity and peripheral speed of the rotor-2 are the same as those of the rotor-1[7]. The preliminary design parameters such as flow angles, camber angles, stagger angles, and degree of reaction are mention in Tables 1 and 2. The detailed design process was discussed by Mistry and Pradeep [7].

2.1 Blade Geometry and Material

The contra-rotating fan rotors for the study are highly twisted and have a 3-dimensional shape for both rotors. For the rotor with an aspect ratio of 3, the blade height is higher compared to its chord. The blades are made up of LM6 aluminum material. The elastic modulus of 71 GPa, Poisson's ratio of 0.33, and mass density of 2650 kg/m^3 were considered for the structural analysis. The chord of blade1 and blade2 is 45mm. The height of the blade is 151 mm. Tip clearance of blade1 and blade2 are 4 mm and 3mm respectively.

Table.1 Geometrical Parameters at Hub, Mean and Tip Section for Rotor-1 [7]

Rotor-1			
Station	**Hub**	**Mean**	**Tip**
β_1 (in degree)	20.90	37.37	48.89
β_2 (in degree)	19.66	1.5	23.35
DOR	0.032	0.517	0.688
Incidence angle (in degree)	2	0	-2
Chamber angle (in degree)	41.35	39.85	31.53
Deviation angle (in degree)	17.85	24.46	21
Stagger angle (in degree)	-1.7	17.43	35.11

Table.2 Geometrical Parameters at Hub, Mean and Tip Section for Rotor-2 [7]

Rotor-2			
Station	**Hub**	**Mean**	**Tip**
β_3 (in degree)	48.27	56.34	61.73
β_4 (in degree)	20.57	39.82	50.65
DOR	0.02	0.56	0.72
Incidence angle (in degree)	2	0	-2
Chamber angle (in degree)	28.69	24.51	20.75
Deviation angle (in degree)	3	7.5	7.67
Stagger angle (in degree)	30	44.08	53.36

3. Analytical Approach

3.1 Bernoulli Euler Beam (Approximation of Rotor Geometry as a Uniform Cantilever Beam)

For the Bernoulli-Euler method, the model must have a constant thickness and width; it is considered as a uniform beam. An accurate approximation of the rotor blade geometry is one of the methods to obtain an analytical solution. Generally, the turbine/compressor/fan blades are not constant thickness due to irregular surfaces. Therefore, the thickness of the beam model is considered as an average thickness of the contra-rotating fan rotor. This average thickness of the rotors is determined by averaging across the width of the rotor and, then averaging this value at fixed bottom, mid-length, and top across the length of the blade [8]. Figure-2 shows the uniform cantilever beam. The calculation of natural frequencies is shown as follows. Using the measurement of the contra-rotating rotor,

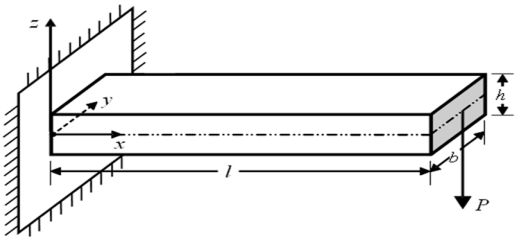

Figure 2 Uniform Cantilever Beam

the average thickness at the fixed bottom of the rotor is determined as;

$$t_{ave-b} = \frac{t_{max-b}+t_{min-b}}{2} \quad (1)$$

similarly, the average thickness at the mid-length of the rotor is;

$$t_{avg-m} = \frac{t_{max-m}+t_{min-m}}{2} \quad (2)$$

at the top (tip) of the rotor, the average thickness is:

$$t_{avg-t} = \frac{t_{max-t}+t_{min-t}}{2} \quad (3)$$

then, the average thickness of the rotor is determined as:

$$t_{avg} = \frac{t_{avg-b}+t_{avg-m}+t_{avg-t}}{3} \quad (4)$$

These average thicknesses of the rotor serve as the uniform thicknesses of the uniform cantilever beam models. It is not necessary to determine the average width (b) of the rotor, since it is nearly constant along the entire rotor length. With these available dimensions, the cross sectional area of the beam can be obtained by $A = t_{avg}b$ and the moment inertia of the beam is $I = \frac{1}{12}bt_{avg}^3$ for the rectangular cross section.

For a uniform cantilever beam subjected to free vibration, the system is considered as a continuous system in which the beam mass is considered as distributed along with the stiffness of the shaft. Then the equation of motion is;

$$\frac{d^2}{dx^2}\left\{ EI(x)\frac{d^2Y(x)}{dx^2}\right\} = \omega^2 m(x)Y(x) \quad (5)$$

$$\text{At } x = 0, Y(x) = 0, \frac{dY(x)}{dx} = 0 ,$$

$$\text{At } x = l, \frac{d^2Y(x)}{dx^2} = 0, \frac{d^3Y(x)}{dx^3} = 0 \quad (6)$$

For a uniform beam under free vibration from equation (5), we obtain

$$w\frac{d^4Y(x)}{dx^4} - \beta^4 Y(x) = 0, \quad (7)$$

Where $\beta^4 = \frac{\omega^4 m}{EI}$

The mode shapes for a continuous cantilever beam is given as

$$f_n(x) = A_n\{(\sin\beta_n L - \sinh\beta_n L)(\sin\beta_n x - \sinh\beta_n x) + (\cos\beta_n L - \cosh\beta_n L)(\cos\beta_n x - \cosh\beta_n x)\}$$

$$n = 1,2,3, \ldots\ldots\infty \text{ and } \beta_n L = n\pi \quad (8)$$

Natural frequency ω_{nf}, from the above equation of motion and boundary conditions can be written as,

$$\omega_{nf} = a_n^2\sqrt{\frac{EI}{\rho AL^4}} \quad (9)$$

$$\text{where } a_n = 1.875, 4.694, 7.885. [9]$$

Here ω_{nf} , ρ and L represent nth natural frequency, density of the material, and length of the beam.

Natural frequency for rotor-1 and rotor-2 obtained from Bernoulli Euler Beam method is listed in Tables 3 and 4. Natural frequencies are obtained up to the third mode for both the rotors. All the three modes of the natural frequency for rotor-1 and rotor-2 are flexural

Table.3 Natural Frequencies of Rotor-1 Obtained from Analytical Solution

Rotor-1		
Mode	**Frequency (Hz)**	**Types of mode**
1	181.39	1st Flexural
2	1136.02	2nd Flexural
3	3182.59	3rd Flexural

Table.4 Natural Frequencies of Rotor-2 Obtained from Analytical Solution

Rotor-2		
Mode	**Frequency (Hz)**	**Type of mode**
1	157.82	1st Flexural
2	987.42	2nd Flexural
3	2764.85	3rd Flexural

4. Modal Analysis of Contra-Rotating Fan Stage

Rotating flexible structures as the fan rotors are often considered as a rotating cantilever beam. The procedure followed by ANSYS to perform modal analysis of non-rotating and rotating fan rotors was discussed in the above sections. To perform the modal analysis following steps were performed.

- Modeling of 3D blade geometry of contra-rotating fan rotor in solid works
- The 3D solid model generated above is used to perform the FE analysis using ANSYS.
- Modal analysis and modal pre-stressed analysis is performed using ANSYS to obtain natural frequencies and mode shapes.

4.1 Meshing of fan rotor blades:

The solid 3D model of the fan rotor was generated using SOLIDWORKS. The model was meshed for both rotors using the ANSYS meshing tool called as Hex-Dominant Mesher as shown in Figure-3. The processing phase solves the equations for these nodes and obtains the results. Meshing is the most important part of structural analysis as an effect of analysis which depends on meshing for this type of highly 3-dimensional geometry. The element is known as performing well when it comes to stress analysis in structures and solid mechanics (ANSYS, 2015). For the present analysis, the highly fine mesh was selected. Rotor-1 and rotor-2 are comprised of 40540 and 42550 elements respectively.
The effect of mesh size was verified such that as the number of elements increases the natural frequencies slightly increase.

(a) Rotor-1 (b) Rotor-2

Fig. 3 Meshing of Contra-Rotating Fan Rotors

4.2 Modal Analysis Considering Stationary Rotor

The modal analysis was carried out to find out the fundamental vibration modes of the rotor blades. This result was used to check the possibility of resonance. All the degrees of freedom presented at the root of the rotor blades are constrained. The blade root is considered as a fixed boundary condition. The FE model was used to obtain the natural frequencies and mode shapes for the contra-rotating fan rotors in a stationary reference frame. The natural frequencies of the rotor-1 and the rotor-2 obtained through analysis are listed in Tables 5 and 6. The mode shapes observed for stationary fan rotors are flexural, torsional, and compound (combining of flexural and torsional modes), respectively. Results are validated with the semi-analytical results obtained by solving equation (9) and they are compared to be matched well. The vibration analysis permits us is to understand not only flexural mode but also torsional mode [10]. Mode shapes of rotor-1 have shown in Figure-4.

Table.5 Modal Analysis of Rotor-1

Rotor-1		
Mode	**Frequency(Hz)**	**Types of mode**
1	179.9	1st Flexural
2	793.01	Flexural +Torsion
3	1088	2ndFlexural
4	1938.8	1st Torsional
5	2575.8	2nd Torsional
6	3200.9	3rd Flexural

Table.6 Modal Analysis of Rotor-2

Rotor-2		
Mode	**Frequency(Hz)**	**Types of mode**
1	153.6	1st Flexural
2	803.88	Flexural +Torsion
3	955.88	2nd Flexural
4	1782.8	1st Torsional
5	2435.8	2nd Torsional
6	2811.9	3rd Flexural

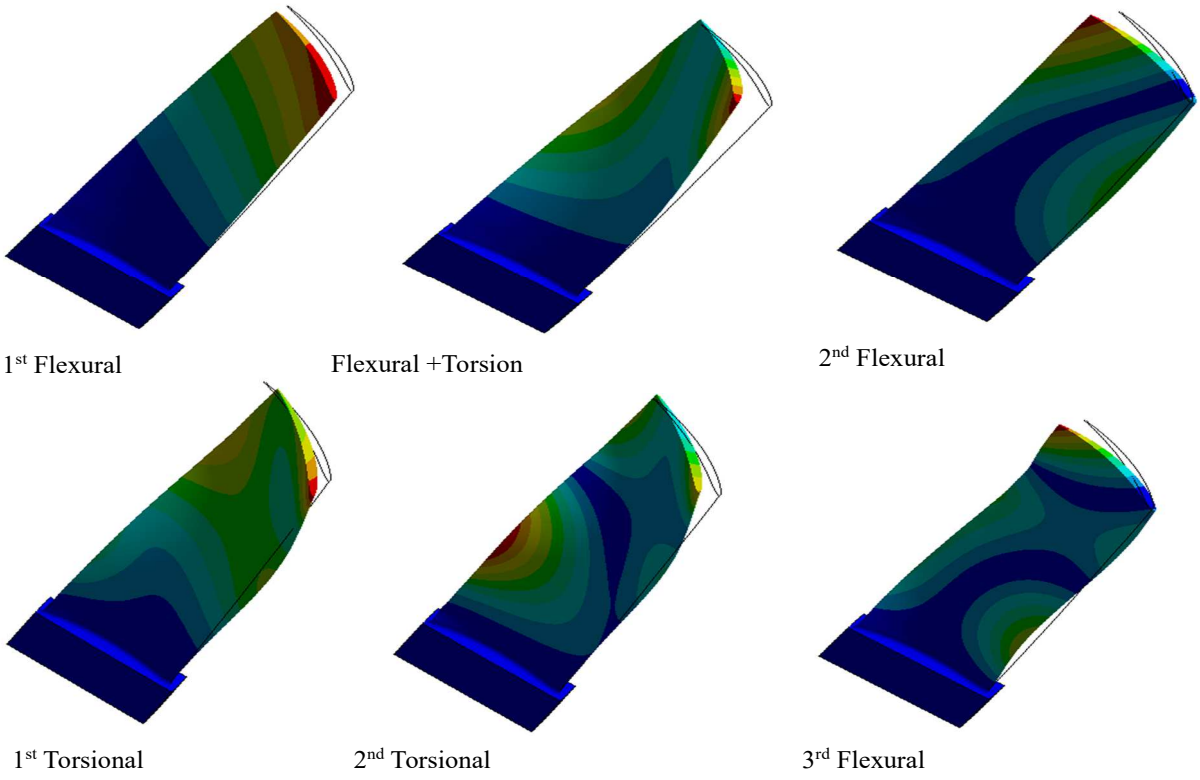

Figure 4 Mode Shapes of the Non-Rotating Fan Rotor-1

Table.7 Compression of Natural Frequencies for A Non-Rotating rotor-1

Rotor-1		
Mode	**Analytical**	**ANSYS**
1st Flexural	181.39	179.9
2nd Flexural	1136.02	1088
3rd Flexural	3182.59	3200.9

Table.8 Compression of Natural Frequencies for A Non-Rotating rotor-2

Rotor-2		
Mode	**Analytical**	**ANSYS**
1st Flexural	157.82	153.6
2nd Flexural	987.42	955.88
3rd Flexural	2764.85	2811.9

The result of the natural frequencies obtained from the analytical solution and FEM analyses for rotor 1 and rotor-2 are compared from Tables 7 and 8. It can be found the results that all the flexural modes of the 1st, the 2nd, and the 3rd modes are matched well between the two results.

4.3 Modal Pre-Stressed Analysis Considering Rotating Blades

For an air application in rotating blades, it is necessary to consider the effect of rotation on blade stress. Modal pre-stress analysis helps in understanding the centrifugal load effect. It was found from the experiments that by increasing the rotational speed of rotor-2, the performance of the stage improves [11]. This result demand for carrying out the modal pre-stress analysis considering different speeds. The design speeds of both rotors are 2400-2400 rpm. Due to the rotational speed, the blade centrifugal force acts radially outward. A rotating blade has larger stiffness than a stationary blade because a rotation leads to a stiffening effect due to the centrifugal force, which depends on the rotational speed of the fan blade. The centrifugal force, which produces tensile stress on the rotor blade increases stiffness. An increase in stiffness leads to an increase in the natural frequency of the rotor blade. For the modal pre-stress analysis, the static analysis was performed before the modal analysis. Modal analysis of rotating structures through FEA is performed considering the rotor dynamic effect. In pre-stressed modal analysis, the rotational speed is given as inertial velocity (rad/s) for all elements in static analysis. These results are then used in the modal analyses. FE

model of a rotating beam is developed in ANSYS. The analysis using ANSYS was performed at different rotational speeds are listed in Tables 9 and 10. Mode shapes of the rotor1 blade obtained from the FEM analysis for 2400 rpm are presented in Figure-5. Mode shapes are also computed for different rotational speeds at 2400rpm(40Hz), 3000 rpm (50 Hz), 3600 rpm (60 Hz), 4200 rpm (70 Hz), and 4800 rpm (80 Hz) respectively of the rotor-1 and rotor-2. It is observed that the nature of these mode shapes is marginally affected by the rotating speeds. The mode shapes observed from the stationary fan rotors are flexural, torsional, and compound (combining of flexural and torsional) modes respectively. Mode shapes of rotor-1 are shown in Figure 5.

As compared with the non-rotating case, it can be seen from Tables 9 and 10 that the natural frequency increases with increasing rotational speed. Tables 9 and 10 show the natural frequencies at different rotational speeds have been obtained and it is observed that increase in natural frequencies.

5. Analysis of Contra-Rotating Fan Rotors

The structural Analysis of contra-rotating fan rotor blades was carried out using ANSYS 14.0. In the analysis, the single blade of both rotors of the contra-rotating fan was considered along with the base. Structural analysis was carried out to determine the mechanical stress and deformation experienced by the contra-rotating fan blades. To perform this analysis, one way transfer FSI was used for which the pressure load achieved by CFD analysis, was used to accomplish FE analysis.

5.1.1 CFD Analysis of Contra-Rotating Fan

CFD analysis of the contra-rotating fan stage is performed by ANSYS CFX. The CFD analysis has done for a single passage through the combinations of both rotors and it was assumed to represent the flow situation for the entire fan rotors combination. Computational domain for CFD analysis consisted of

Table.9 Modal Pre-stress Analysis of Rotor-1 with Different Rotational Speed

Natural Frequencies (Hz)						
Mode	**0 rpm**	**2400 rpm**	**3000 rpm**	**3600 rpm**	**4200 rpm**	**4800 rpm**
1F	179.9	183.51	188.14	193.7	197.22	201.19
2F	793.01	796.56	817.72	822.95	826.28	830.07
1T	1088	1091	1107.2	1110.6	1113.1	1115.9
1EB	1938.8	1941.6	1997.2	2000.6	2002.9	2005.4
2T	2575.8	2581.8	2624.8	2631.5	2635.8	2640.7
2EB	3200.9	3206.2	3248.5	3254.6	3258.6	3263.2

Table.10 Modal Pre-stress Analysis of Rotor-2 at the Different Rotational Speed

Natural Frequencies (Hz)						
Mode	**0 rpm**	**2400 rpm**	**3000 rpm**	**3600 rpm**	**4200 rpm**	**4800 rpm**
1F	153.6	160.99	164.89	169.52	174.82	180.72
2F	803.88	810.81	814.13	818.11	822.71	827.87
1T	955.88	959.74	961.93	964.64	967.89	971.87
1EB	1782.8	1787.40	1788.7	1790.4	1792.3	1794.5
2T	2435.8	2445.30	2449.6	2454.8	2460.8	2467.5
2EB	2811.9	2818.80	2821.7	2825.1	2829.3	2834

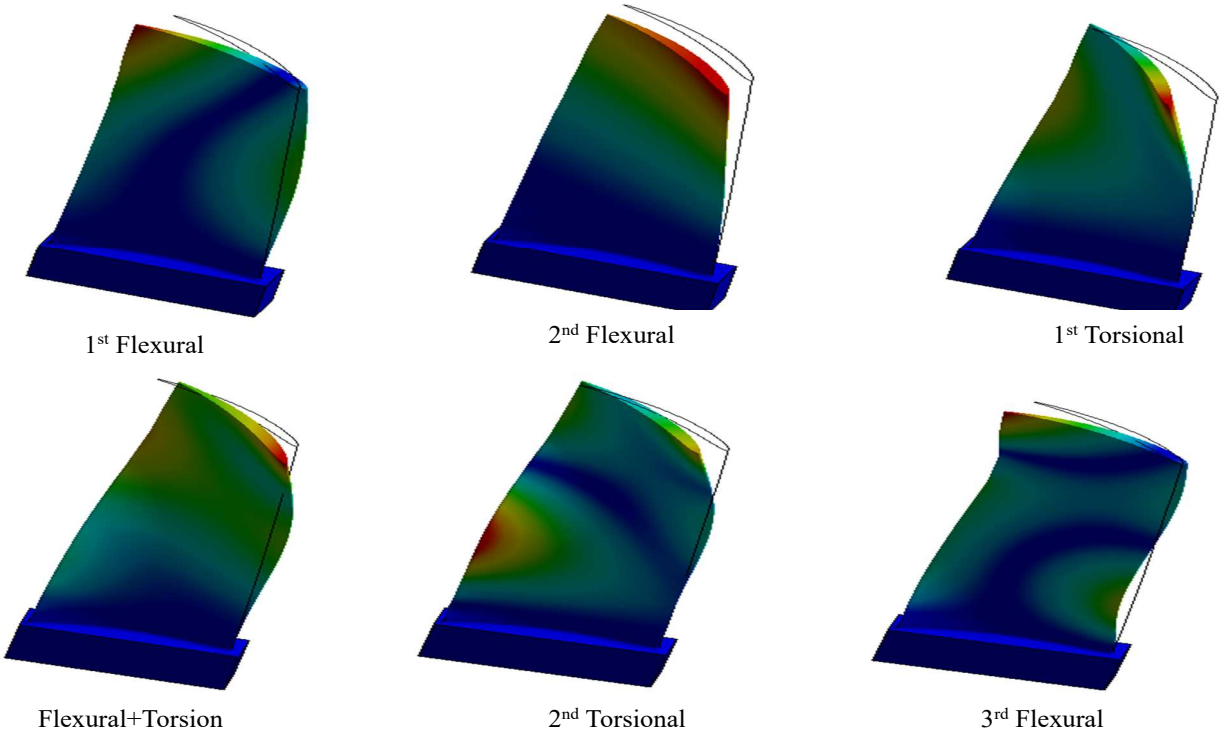

Figure 5 Mode Shapes of Rotating Fan Rotor-1

the single blade flow passage of the contra-rotating fan rotors is shown in Figure-5. The computational domain is split into two parts as, the rotating CFD analysis of the contra-rotating fan stage is performed by ANSYS CFX. The CFD analysis has done for a single passage through the combinations of both rotors and it was assumed to represent the flow situation for the entire fan rotors combination. The computational domain for CFD analysis consisted of the single blade flow passage of the contra-rotating fan rotors is shown in Figure-6. The computational domain is split into two parts as, the rotating domain for rotor-1 and the rotating domain for rotor-2. Both domains are connected with the "frozen rotor" type of interface model. The length of the contra-rotating rotor-1 domain is assumed such that the rotating disk on which the rotor is placed has a thickness of 10 mm from the leading edge of a hub and the inlet of the rotor-1 is placed at one chord upstream from this distance. Based on the axial spacing between the two rotors, the half region is covered in domain-1 to obtain the rotor-1 exit parameter. Domain for rotor-2 is generated by placing the inlet of domain-2 at the exit of the rotor-1 domain. The exit of domain-2 is placed as 10mm disk thickness plus 2 chords downstream as reported in reference [12].

5.1.2 Grid Generation

The computational grid for CFD analysis is generated using ANSYS Turbo.Grid. This inbuilt grid generator has a provision to generate an automated grid for a. specified geometry. For maintaining the tip gap, the topology feature is available to maintain the specified tip clearance as per the requirement of 3mm for rotor-

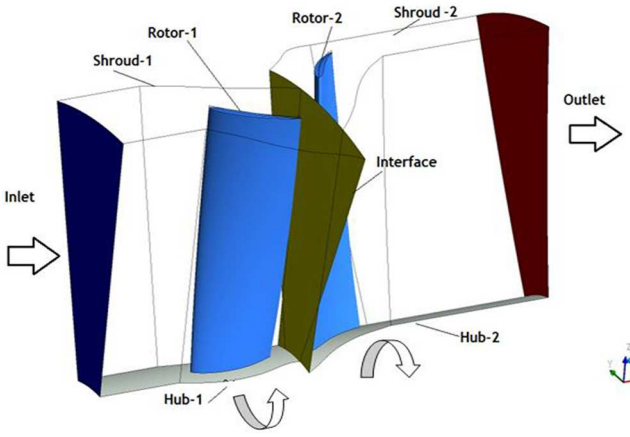

Figure 6 Computational flow domain

1 and 3.5 mm for rotor-2. The topology feature is a structure .of blocks that act as a framework for positioning mesh elements, Hexahedral (Hex) elements [8]. They are laid out adjacently.to each

other, without overlaps or gaps at the corner between. adjacent blocks with which, the entire domain is filled.

5.1.3 Boundary Conditions

The boundary conditions are considered as design conditions such as an inlet velocity profile achieved from the experiment and the static pressure outlet condition. The boundary conditions are specified in an absolute frame of the reference. The shear stress transport (SST) model for turbulence is utilized for its advantage in simulating the variations in Reynolds's stresses due to the Coriolis forces presented in rotating frames of reference.

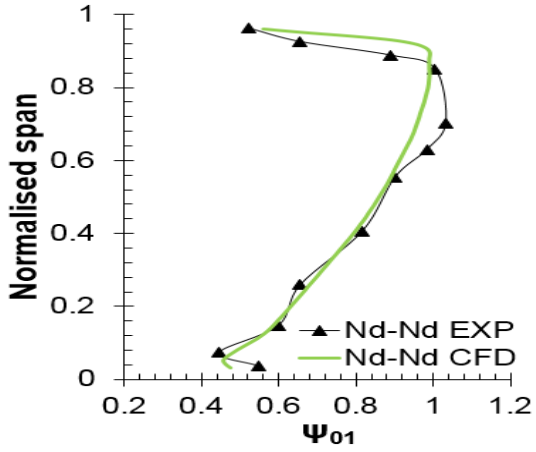

(a) Rotor-1

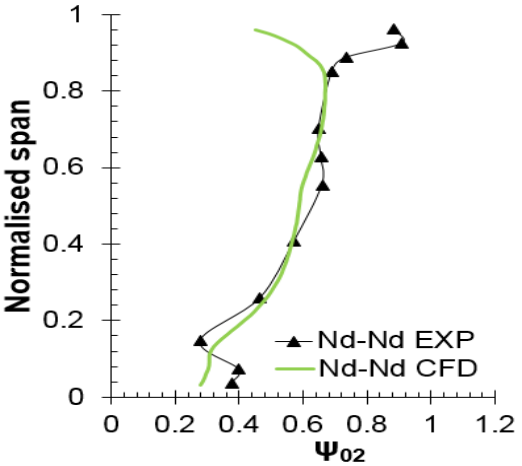

(b) Rotor-2

Fig.7 CFD Validation of Total Pressure Coefficient for (a) Rotor-1 (b) Rotor-2 [13]

Figure-7 shows the validation of total pressure rise coefficient variation along the span at design mass flow rate for design speed combinations. It can be observed that the total pressure coefficient of the contra-rotating rotor-1 matches well within 50 % of its span and thereafter, it shows a lower magnitude of about 2 to 4 % compared with the experimental results. This is due to the higher negative incidence near that region and subsequently, it is unable to capture the flow field in that location. The rotor-2 shows a variation of the total pressure coefficient along the entire span. Specifically, near the tip, the region shows a lower magnitude compared with the experimental results [13]. The results are validated by showing good agreements. Base on this validation the computational results are used for further structural analysis.

6. Structural Analysis

A one-way FSI analysis has been performed in this paper. CFD analysis producing static pressure on both suction and pressure surfaces has been considered as loads on the contra-rotating fan stage at different speeds and mass flow rates. Deformation and Von-Misses stress are obtained from the structural analysis at two mass flow rates (design and stall) and for two different speed combinations (2400-2400 and 2400-2600 rpm). Pressure, deformation, and Von-Misses stress of the rotor-1 and rotor-2 at 2400-2400 rpm with mass flow rates of 6 kg/sec have been imported for the analysis. These imported results are shown in Fig. 8 and 9.

Figure-8(a) shows the contour of the pressure load acting on rotor-1 imported from CFD analysis at mass flow rate 6 kg/sec and speed combination of 2400-2400 rpm. There are three components of the force generated by the high speed air on the fan blade. These components are tangential force (F_t) and axial force (F_a) and centrifugal force (F_c). The axial, tangential, and centrifugal components of forces acting on the blade are considered as loads to investigate the structural response of rotor-1. Sum of the force components obtained from CFD analysis for the one-way FSI are listed in Table 11 and 12.

Table.11 Force on Rotor-1 at Design Mass Flow Rate.

Rotor-1		
Design mass flow rate	6 kg/sec	6 kg/sec
Speed combination	2400-2400 rpm	2400-2600 rpm
Axial force (F_a)	4.43 N	3.56 N
Tangential forces (F_t)	6.06 N	6.37 N
Centrifugal Force (Fc)	7.18 N	15.43 N

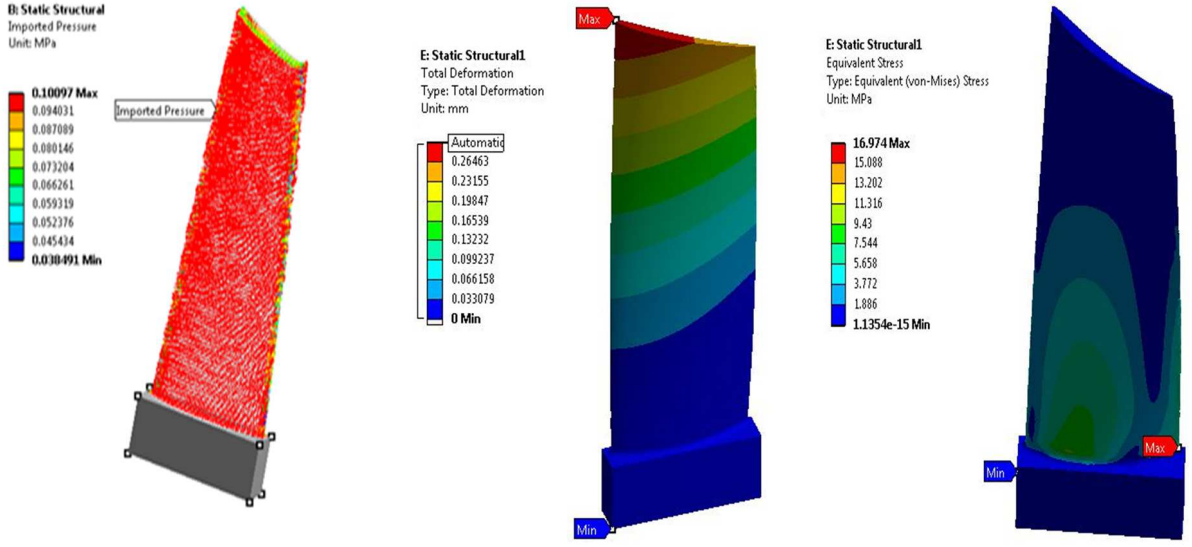

(a) Imported Pressure (b) Imported Pressure (c) Stress Distribution

Figure 8 Imported Pressure, Deformation and Stress Contour of Rotor-1

Table. 12 Forces on Rotor-1 at Stall Mass Flow Rate

Rotor-1		
Stall mass flow rate	5.3 kg/sec	5.3 kg/sec
Speed combination	2400-2400 rpm	2400-2600 rpm
Axial force(F_a)	3.50 N	3.34 N
Tangential forces(F_t)	6.50 N	6.39 N
Centrifugal Force(Fc)	15.49 N	15.50 N

It may be observed from Table-12 that an increase of speed of rotor-2, increases the centrifugal force from 7.18N to 15.43N. It is also observed that increment of the speed ratio does not affect the axial and tangential forces significantly. Similar improvement of pressure rise in contra-rotating fan stage has been reported in the literature [14].

Figure-8(b) presents the deformation contour of contra-rotating fan rotor-1. It is observed that the maximum deformation is 0.297 mm, occurs at the tip section near the leading edge of the contra-rotating fan blade. Minimum deformation occurs at the root section as rotor connected with a fixed support at the root. This indicates the higher aerodynamic loading of rotor-1 at the tip as per the design and experimental results are shown in Figure-7. Figure-8(c) shows the stress distribution contour of rotor-1. It is observed that the maximum stress of 16.97 MPa occurs at the root section on the pressure side of the contra-rotating fan blade while minimum stress occurs at the tip section. An asymmetry of deformation and stress patterns is observed due to the asymmetry of pressure loading with respect to the elastic axis of the rotor blades. At speed combination 2400-2600 rpm, maximum deformation is 0.312 mm and maximum von-misses stress is 16.04 MPa. It is also observed that maximum deformation is at the rotor tip and maximum stress is near the root of the rotor. The result of the structural analysis is listed in Table 13.

Table .13 FE Analysis of Rotor-1 at Design Mass Flow Rate

Rotor 1		
Speed combination	2400-2400 rpm	2400-2600 rpm
Design mass flow rate	6 kg/sec	6 kg/sec
Maximum Von-Misses stress	16.97 MPa	16.04 Mpa
Maximum Deformation	0.297 mm	0.312 mm

Table 14 shows the results of the structural analysis of rotor-1 in terms of Von-Misses stress and deformation at stall mass flow rate of 5.3 kg/sec with different speed combinations of 2400-2400 and 2400-2600 rpm. It is observed that at 2400 rpm maximum stress is 17.89 MPa and maximum deformation is 0.317 mm. At rotational speed 2600 rpm, maximum stress is 17.96 MPa and maximum deformation is 0.301 at the tip of the blade near the leading edge. This is because of the rapid change in the pressure gradient at the tip of the blade due to fluid pressure. The location of maximum deformation is near the leading edge at the tip of the rotor, because the leading edge is the region of high energy impact which leads to maximum deformation.

Table.14 FE analysis of Rotor-1 at Stall Mass Flow Rate

Rotor 1		
Speed combination	2400-2400 rpm	2400-2600 rpm
Stall mass flow rate	5.3 kg/sec	5.3 kg/sec
Maximum Von-Misses stress	17.89 MPa	17.96 MPa
Maximum Deformation	0.317 mm	0.301 mm

Similarly, the pressure load on rotor-2 is imported from CFD analysis to FE analysis through one-way FSI at a design mass flow rate of 6 kg/sec speed combination of 2400-2400 rpm. Figure-9(a) shows the imported pressure load on contra-rotating fan rotor-2 from CFD analysis to obtain the deformation and Von-Misses stress. There are three components of the force generated by the high speed air on the fan blade. These components are tangential force (F_t) and axial force (F_a) and centrifugal force (F_c). The axial, tangential, and centrifugal forces acting on the rotors are considered to obtain the deformation and Von-Misses stress. It may be noted here that, the already pressurized air through rotor-1 gets transferred to rotor-2 through the suction effect of rotor-2. The high pressure air supplied to rotor-2 results into higher aerodynamic load on rotor-2. The forces obtained from CFD analysis through one way FSI at different speed combinations and mass flow rates are tabulated in Tables 15 and 16.

Table.15 Forces on Rotor-2 at Design Mass Flow Rate

Rotor-2		
Design mass flow rate	6 Kg/sec	6 Kg/sec
Speed combination	2400-2400 rpm	2400-2600 rpm
Axial force(F_a)	613.62 N	615.2 N
Tangential forces(F_t)	1001.8 N	1006 N
Centrifugal Force(Fc)	208.48 N	209.35 N

Table.16 Forces on Rotor-2 at Stall Mass Flow Rate

Rotor-2		
Stall mass flow rate	5.3 Kg/sec	5.3 Kg/sec
Speed combination	2400-2400 rpm	2400-2600 rpm
Axial force(F_a)	615.75 N	616.66 N
Tangential forces(F_t)	1006.5 N	1008 N
Centrifugal Force(Fc)	209.43 N	209.74 N

Figure-9(b)shows the deformation of aerodynamically loaded contra-rotating fan rotor-2. It is observed that the maximum deformation of 4.37 mm occurs at the tip section near the leading edge of the contra-rotating fan blade and minimum deformation occurs at the root section. The deformation patterns observed in the rotor blades show combined bending and torsion of the blades with a different ratio of resultant longitudinal to torsional force. Figure-9(c) shows the contour of stress distribution on the rotor blade due to the application of loads. It is observed that the maximum stress of 2100.9 MPa occurs at the root section on the pressure side of the contra-rotating fan blade, and minimum stress occurs at the tip section. An asymmetry of stress patterns is also observed due to the asymmetry of pressure loading. The maximum deformation observed is 4.47 mm and the maximum von-misses stress is 2217.8 MPa at a speed combination of 2400-2600 rpm. It was also observed that maximum deformation is at the tip of the rotor and maximum stress is near the root of the rotor. The result of structural analysis has been tabulated in Table 17.

Table.17 FE analysis of Rotor-2 at Design Mass Flow Rate

Rotor 2		
Speed combination	2400-2400 rpm	2400-2600 rpm
Design mass flow rate	6 kg/sec	6 kg/sec
Maximum Von-Misses stress	2100.9 MPa	2217.8 MPa
Maximum Deformation	4.37 mm	4.47 mm

The Finite Element analysis for rotor-2 at stall mass flow rate of 5.3 kg/sec and speed combination of 2400-2400 rpm shows that the maximum deformation is 4.46 mm and maximum Von-Misses stress is 2302 MPa at a speed combination of 2400-2600 rpm. The maximum deformation is 4.45 mm and the maximum Von-Misses stress is 2278.3 MPa at a speed combination of 2400-2600 rpm. From the deformation and von-misses stress contour, it was also observed that maximum deformation is at the tip of the blade and maximum stress is near the root of the blade. The result of structural analysis has been tabulated in Table 18.

Table.18 FE analysis of Rotor-2 at Stall Mass Flow Rate

Rotor 2		
Speed combination	2400-2400 rpm	2400-2600 rpm
Stall mass flow rate	5.3 kg/sec	5.3 kg/sec
Maximum Von-Misses stress	2302 MPa	2278.3 Mpa
Maximum Deformation	4.46 mm	4.45 mm

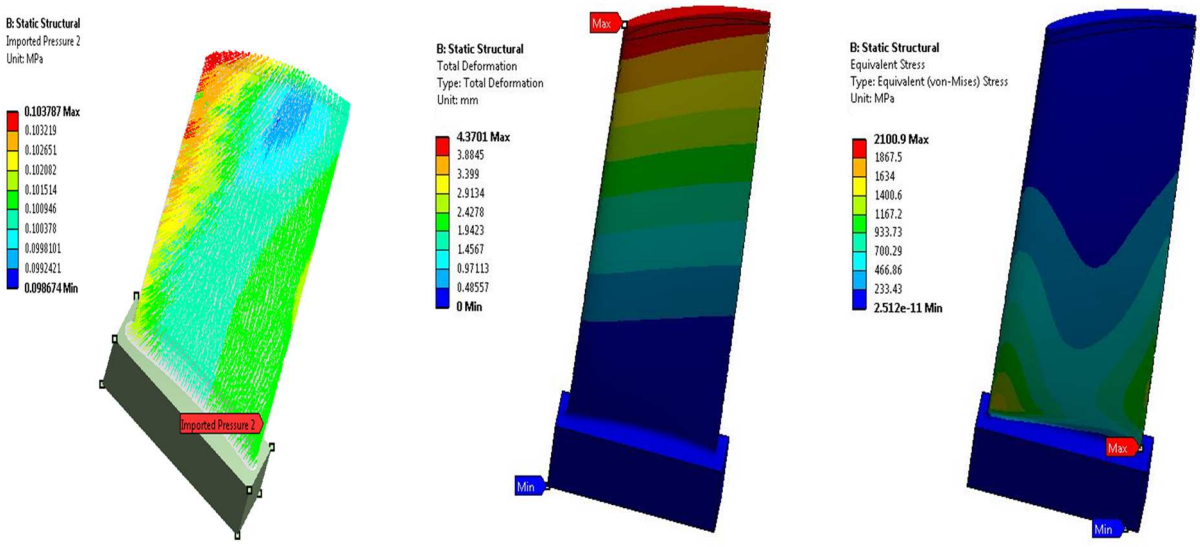

(a) Imported Pressure (b) Deformation (c) Stress Distribution

Figure 9 Imported Pressure, Deformation, and Stress Distribution of Rotor-2.

7. Conclusion

The present study discusses the vibration and structure analyses of the contra-rotating fan stage. One way fluid-structure interaction has been carried out for the contra-rotating fan stage. The computational analysis of the contra-rotating fan stage has been performed using ANSYS CFX. Based on the results obtained from the CFD analysis, deformation and Von-Misses stress have been obtained from the structural analysis at design and stall mass flow rates for two different speed combinations (2400-2400 and 2400-2600 rpm). Modal analysis and modal pre-stress analysis (due to rotation) have been carried out to obtain the natural frequencies of the contra-rotating fan stage. Some of the important conclusions derived based on the present computational and analytical analysis are

- Bernoulli-Euler Beam method was used as an analytical approach to finding the natural frequencies of the blade. The frequency analysis carried out using ANSYS FE Tool shows a reasonably good match with analytical calculation. For the first, second, and third flexural modes of vibration, the natural frequencies and the mode of vibration slightly resembles the analytical solution.
- Centrifugal force due to rotation causes pre-stressing in the blade which leads to an increase in stiffness and natural frequency.
- The modal pre-stress analysis shows that designed natural frequency (40Hz) doesn't coincide with natural frequency for both the rotors so it minimizes the chance of resonance.
- CFD pressure was imported to the FE analysis through one way transfer FSI and considered as a load to perform structural analysis to obtain maximum deformation & maximum Von-Misses stress.
- The contours of stress distribution show the location of the maximum stress is near the root area of the blades and the location of minimum stress is at the tip section close to the leading edge.
- Asymmetric distributions of deformation and stress have been noticed resulting from the asymmetric pressure loading with respect to the elastic axis of the rotor blades.
- Rotor-2 is aerodynamically highly loaded which causes higher deformation near the leading edge at the tip region and has high Von-Misses stress near the root.

Nomenclature

β - Relative flow angle	α - Absolute flow angle
Station 1- Inlet of rotor-1	Station 2- Exit of rotor-1
Station 3- Inlet of rotor-2	Station 4- Exit of rotor-2

Acknowledgment

We thank the Department of Aerospace Engineering, Indian Institute of Technology Kharagpur for supporting us to carry out the research.

References

[1] C.S. Mistry, A.M. Pradeep, Study of the velocity flow field under distorted inflow conditions for a high aspect ratio low speed contra rotating fan, in: Proceedings of the 2013 ASME GT India Conference, Bangalore, Paper no. GTIndia2013-3594, 2013.

[2] Jacobus Dani¨el Brandsen "Prediction of Axial Compressor Blade Vibration by Modelling Fluid-Structure Interaction"December 2013

[3] B Roy, K Ravibabu, P Shrinivasa Rao, S Babu, A Raju and P N Murthy,1992, " Flow studies in ducted twin-rotor Contra rotating axial flow fans.", International Gas Turbine and Aero engine congress and exposition, Germany, June 1-4,92-GT-390

[4] Jian Xu, Chunqig Tan, Haisheng Chen,Yagnli Zhu and Dongyang Zhang, " Influence of tip clearance on performance of a contra rotating fan", *Journal of Thermal Science*,Vol-18,No-3,pp 207-214.

[5] Benra, Friedrich-Karl, et al. "A comparison of one-way and two-way coupling methods for numerical analysis of fluid-structure interactions." Journal of applied mathematics 2011 (2011).

[6] A. Timperi, "Fluid-structure interaction calculations using a linear perturbation method," in Proceedings of the 20th International Conference on Structural Mechanics in Reactor Technology (SMiRT '09), 2009.

[7] CS Mistry, AM Pradeep "Design and performance analysis of a low-speed, high aspect ratio contra-rotating fan stage"The 11th Asian International Conference on Fluid ..., 2011

[8] Inoyama, Daisaku. "Vibration analysis of a fan/compressor blade." (2003).

[9] Rao, S. S., "Mechanical Vibration," 3rd edition, Addison-Wesley, 1995

[10] Mohan, R. S., A. Sarkar, and A. S. Sekhar. "Vibration analysis of a steam turbine blade." INTER-NOISE and NOISE-CON Congress and Conference Proceedings. Vol. 249. No. 7. Institute of Noise Control Engineering, 2014.

[11] Mistry, Chetan S., and A. M. Pradeep. "Investigations on the effect of inflow distortion on the performance of a high aspect ratio, low speed contra rotating fan stage." ASME Turbo Expo-2013, San Antonio, Texas, USA, Paper No-GT2012-94311 (2013).

[12] Mistry,C.S., " Experimental investigations on performance of contra rotating fan stage under clean and distorted inflow conditions",2014, PhD thesis, IIT Bombay

[13] Nayak, Nikhil, and Chetan Mistry. "Criteria for selection of solidity in design of contra rotating fan stage." NAPC-2017, March: 15-17.

[14] Pundhir, D. S., and P. B. Sharma. "A Study of aerodynamic performance of a contra rotating axial compressor stage." *Defence Science Journal* 42.3 (1992): 191.

[15] Chen, Y. Y., et al. "A study of speed ratio affecting the performance of a contra-rotating axial compressor." Proceedings of the Institution of Mechanical Engineers, Part G: *Journal of Aerospace Engineering* 222.7 (2008): 985-991.

[16] Gao, Limin, et al. "The effect of speed ratio on the first rotating stall stage in contra-rotating compressor." Turbo Expo: Power for Land, Sea, and Air. Vol. 44748. American Society of Mechanical Engineers, 2012. of Mechanical Engineers, 2012.

[17] Srinivasan, A. V. "Flutter and resonant vibration characteristics of engine blades: An igti scholar paper." ASME 1997 International Gas Turbine and Aeroengine Congress and Exhibition. American Society of Mechanical Engineers, 1997.

[18] Sharma, P. B., Y. P. Jain, and D. S. Pundhir. "A study of some factors affecting the performance of a contra-rotating axial compressor stage." *Proceedings of the Institution of Mechanical Engineers*, Part A: Power and Process Engineering 202.1 (1988): 15-21.

[19] Ramamurti, V., and R. Kielb. "Natural frequencies of twisted rotating plates." *Journal of Sound and Vibration* 97.3 (1984): 429-449.

[20] Genta, Giancarlo. *Dynamics of rotating systems*. Springer Science & Business Media, 2007.

Supen Kumar Sah is a Ph.D. scholar in the Department of Aerospace Engineering, IIT Kharagpur, India. He has completed B.Tech in Mechanical Engineering from CET Bikaner, India. He received his M.Tech from IIT Kharagpur, India. His area of research includes Advanced Composite Structures, Functionally Graded Materials.

Dr. Anup Ghosh is an Associate Professor in the Department of Aerospace Engineering, IIT Kharagpur, India. He has done B.Tech in Civil Engineering from Jalpaiguri Government Engineering College. He received his M.E. from B.E. College (D.U.) Howrah, India, and Ph.D. from IIT Kharagpur, India. His area of research

is: Advanced Composite Structures, Fracture control of CFRP laminated composite, Smart Composite Materials,

Dr.Chetan S. Mistry is an Assistant Professor in the Department of Aerospace Engineering, IIT Kharagpur. He has done his graduation in Mechanical Engineering from REC, Surat (Presently NIT-Surat). He received M.E.in Turbo Machinery from NIT, Surat; Ph.D. from IIT Bombay. His area of research is design and performance augmentation strategies for turbomachines, experimental and CFD study of turbomachines, contra rotating axial flow turbomachines aerodynamics, electric propulsion as well as fluid mechanics & heat transfer, and experimental aerodynamics.